Experiment and simulation on mechanical behavior in 1/2-scale demonstration REBCO coil system of Skeleton Cyclotron for cancer therapy

Hiroshi Ueda, Ryota Komae, Aoi Yamashita, Ryota Inoue, SeokBeom Kim, So Noguchi, Tomonori Watanabe, Mitsuhiro Fukuda, Gen Nishijima, Rui Kumagai, Atsushi Ishiyama

***Abstract*— We have introduced the Skeleton Cyclotron, a high-temperature superconducting (HTS) air-core compact cyclotron designed to produce medical radioisotopes (RIs) to be used in targeted alpha-particle therapy, an innovative approach to cancer treatment. The coil system of the Skeleton Cyclotron comprises circular main coils for creating an isochronous field and non-circular sector coils to generate an azimuthally varying field. All of these coils are wound using the REBCO tape with a no-insulation (NI) winding technique, chosen for its ability to provide high current densities and thermal stability. To demonstrate the feasibility of our concept, we developed a half-size prototype called the Ultra-Baby Cyclotron. This prototype includes three pairs of sector coils and four main split coils. To enhance the durability of the coils and protect them from the intense electromagnetic forces involved, we reinforced them with a YOROI-coil (Y-based Oxide superconductor and Reinforcing Outer Integrated coil) structure. In the summer of 2022, we started testing on the Ultra-Baby Cyclotron, and then we conducted measurements of mechanical deformations in the coils. Additionally, we conducted numerical simulations. This study presents the experimental and numerical results regarding the mechanical behaviors of NI-REBCO coils in the Ultra-Baby Cyclotron.**

***Index Terms*— Cyclotrons, high-temperature superconducting magnets, mechanical property, No-insulation coil.**

I. INTRODUCTION

TARGETED alpha-particle therapy represents a novel approach to cancer treatment. In this therapy, a targeted drug labeled with alpha-emitting radioisotopes (RIs) is administered to cancer patients. These targeted drugs naturally accumulate in cancer cells, ultimately causing damage to the cancer cells through the emission of alpha particles. To advance targeted alpha-particle therapy, it's crucial to produce alpha-emitting RIs within facilities located near hospitals due to the short half-lives of these nuclides. Accelerators offer promising solutions to address these challenges [1][2]. To this end, we have introduced the Skeleton Cyclotron, a high-temperature superconducting (HTS) air-core compact cyclotron [3]. The coil system of the Skeleton Cyclotron includes circular main coils for generating an isochronous field and non-circular sector coils for producing an azimuthally varying field. All of these coils are wound using the REBCO tape and the no-insulation (NI) winding technique. This choice is made to achieve both high current densities and thermal stability [4].

We designed and constructed the half-size demonstration NI-REBCO coil system, which we refer to as the Ultra-Baby Cyclotron. This system includes three pairs of sector coils and four main split coils. To enhance the robustness of the Ultra-Baby Cyclotron's coils against the formidable electromagnetic forces, we have reinforced them with a YOROI-coil (Y-based Oxide superconductor and Reinforcing Outer Integrated coil) structure. Our experiments of the Ultra-Baby Cyclotron commenced in the summer of 2022. During this phase, we measured the mechanical deformation of the coils. Additionally, we conducted mechanical simulations. In this study, we report our findings from both the experimental and numerical analyses of the mechanical behavior of NI-REBCO coils within the Ultra-Baby Cyclotron.

II. 1/2-SCALE DEMONSTRATION MODEL

In this study, a 1/2-scale demonstration model of a cryocooler-cooled HTS coil system, called the Ultra-Baby Cyclotron, designed for the Skeleton Cyclotron, was fabricated to investigate its electromagnetic, mechanical, and thermal behaviors [5]. Fig. 1 provides a schematic drawing of the Ultra-Baby Cyclotron, which was specifically designed for accelerating protons up to an energy level of 5 MeV/u. The beam extraction radius is 0.2 m. The coil system of the Ultra-Baby Cyclotron comprises four pairs of circular main coils and three pairs of non-circular sector coils. Tables I and II outline the specifications for the main coils and sector coils, respectively. Fig. 2 displays a photograph of the sector coils

Submitted for review September 26, 2023

The part of this work was supported by JST-OPERA, and JSPS Grant-in-Aid for Scientific Research (S) Grant Number 18H05244. (Corresponding author: Hiroshi Ueda)

Hiroshi Ueda, Ryota Komae, Aoi Yamashita, Ryota Inoue, and SeokBeom Kim are with Okayama University, Okayama 700-8530, Japan (e-mail: hiroshi.ueda@okayama-u.ac.jp).

So Noguchi is with the Graduate School of Information Science and Technology, Hokkaido University, Sapporo 060-0814, Japan.

Tomonori Watanabe is with the Chubu Electric Power Company, Nagoya 459-8522, Japan.

Mitsuhiro Fukuda is with the Research Center for Nuclear Physics, Osaka University, Osaka 567-0047, Japan.

Gen Nishijima is with National Institute for Materials Science, Tsukuba 305-0003, Japan.

Rui Kumagai and Atsushi Ishiyama is with the Department of Electrical Engineering and Bio-science, Waseda University, Tokyo 169 8555, Japan.

Color versions of one or more of the figures in this article are available online at http://ieeexplore.ieee.org

and main coils. These coils are the no-insulation coil, wound with REBCO tape, and co-wound with SUS tape. To protect the coil windings from potential damage caused by the substantial electromagnetic forces involved, the coils within the Ultra-Baby Cyclotron are reinforced with a YOROI-coil structure, as shown in Fig. 3. The YOROI-coil structure integrates REBCO tape with reinforcing outer plates to effectively withstand electromagnetic forces [6]. It achieves this by allocating a significant portion of the electromagnetic force to the reinforcing outer components within the YOROI-coil structure. This helps alleviate the stress imposed on the coil windings, even in cases where the hoop stress surpasses the proof stress of the superconducting wire. Numerous reports have demonstrated that circular coils utilizing the YOROI-coil structure are capable of withstanding substantial hoop stresses [7-9]. In the Ultra-Baby Cyclotron, the material employed for the reinforcing plates and frames is SUS (Stainless Steel).

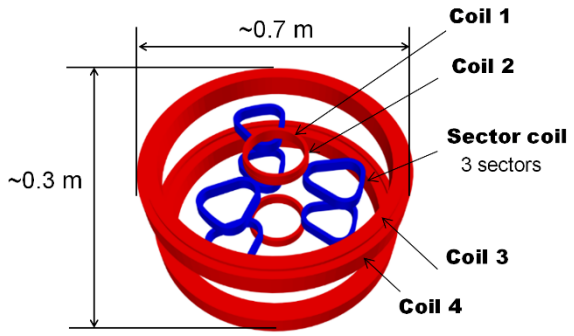

Fig. 1. Schematic drawing of Ultra-Baby Cyclotron.

TABLE I
SPECIFICATIONS OF MAIN COIL.

REBCO tape				
Width (mm)			6	
Thickness (mm)			0.1	
Critical current (A) @ self-field, 77K			200	
	Main Coil 1	Main Coil 2	Main Coil 3	Main Coil 4
Coil i.d (mm)	140.00	160.20	566.26	628.74
Coil o.d (mm)	159.60	161.88	628.66	665.26
Number of turns (each pancake)	50	8	40	51
Number of double pancakes	2	1	4	4
Operating current (A)	540			
Current density (A/mm^2)	367.35	685.71	92.31	201.12

TABLE II
SPECIFICATIONS OF SECTOR COIL

REBCO tape	
Width (mm)	6
Thickness (mm)	0.1
Critical current (A) @ self-field, 77K	200
Coil	
Number of turns / Double pancake	120 (= 60 x 2)
Number of double pancakes	2
thickness of co-winding SUS tape (mm)	0.1
Current (A)	540
Current density (A/mm^2)	423.50

The air-core HTS cyclotron is a novel configuration that has not been previously produced or tested. Detailed observations of the thermal, mechanical, and electromagnetic behavior of the 1/2 scale coil system will be conducted through experiments. Simultaneously, numerical simulations will be carried out to replicate these behaviors and provide insights into the specific phenomena occurring within the coils. The findings from these investigations will inform the design of the full-scale cyclotron.

III. MEASUREMENT OF DEFORMATION OF COILS

A. Experimental setup

Strain gauges have been affixed to the surfaces of the coil winding to measure the strain induced in the longitudinal direction, as shown in Fig. 4. While strain gauges are also placed at additional locations, this experiment focuses on the locations depicted. During the experiments, the coil system is subjected to conductive cooling, gradually reducing the temperature from 300 K to 30 K using a GM cryocooler. All coils are connected in series, and the coil is excited in a stepwise manner with a current sweep rate of 0.07 A/s, reaching a maximum current of 210 A.

In this half-size model, there are six sector coils. As they are non-impregnated and non-circular in shape, deformation may not be uniform across all of them. The primary objective of this study was to observe and analyze the variations in deformation among these sector coils.

B. Experimental results

Fig. 5(a) illustrates the strain results measured in Sector coil #1, showing that strain varies with the operating current. The upper sector coil, SU4-L (left straight section), experienced an increase in strain to 0.35%, resulting in tensile strain. Concurrently, the lower sector coils, SL4-R (right straight

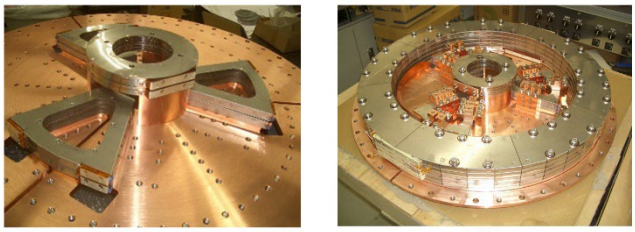

(a) (b)

Fig. 2. Photographs of (a) Sector coils and (b)Main coils.

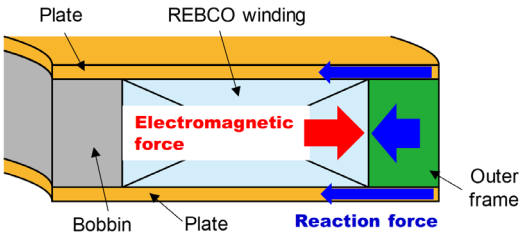

Fig. 3. Principle of YOROI-coil structure

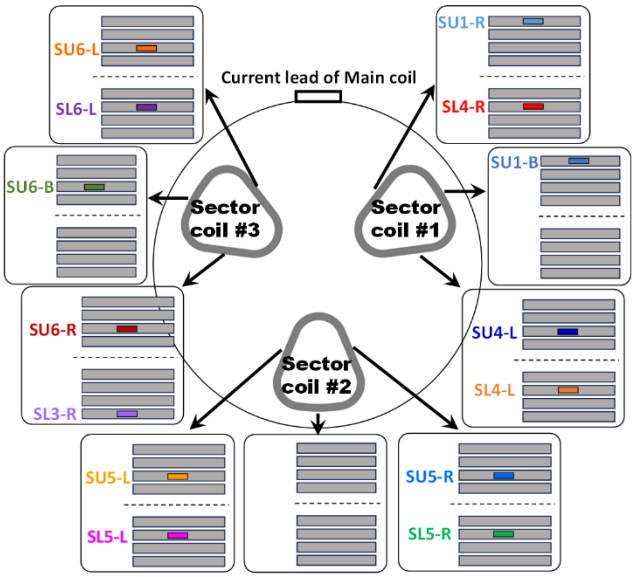

Fig. 4. The locations of strain gauges on surface of sector coils. Strain gauges are also installed at other locations, but the locations observed in this experiment are shown. “SU” represents sector coils above midplane; “SL” represents coils below midplane. "-L", "-R" and “-B” mean the left straight section, the right straight section, and the bottom arc section in a sector coil, respectively.

section) and SL4-L (left straight section), exhibited compressive strain of -0.2% and tensile strains of 0.005%, respectively, indicating asymmetric deformation. The results for Sector coil #2 are presented in Fig. 5(b). In the upper coil, strain changes in SU5 are not stable, but SU5-L experiences tensile strain while SU5-R undergoes compressive strain. Conversely, in the lower coil, both SL5-L and SL5-R exhibit 0.005% tensile strain, suggesting symmetrical deformation. Fig. 5(c) displays the results for Sector coil #3, revealing maximum tensile strain of 0.08% in SL3-R, 0.025% in SL6-L, 0.009% in SU6-L, and -0.0025% in SU6-R. Some strain gauge behavior appears stable, some unstable, and some exhibits significant values. Although strains exceeding the wire degradation allowance of 0.3% were observed, no coil degradation, i.e., no increase in voltage, occurred. These strains are of considerable magnitude and require revalidation. The excitation was stopped at a current of 210 A when strain of 0.35% was observed. Degradation may be observed with further increases in current.

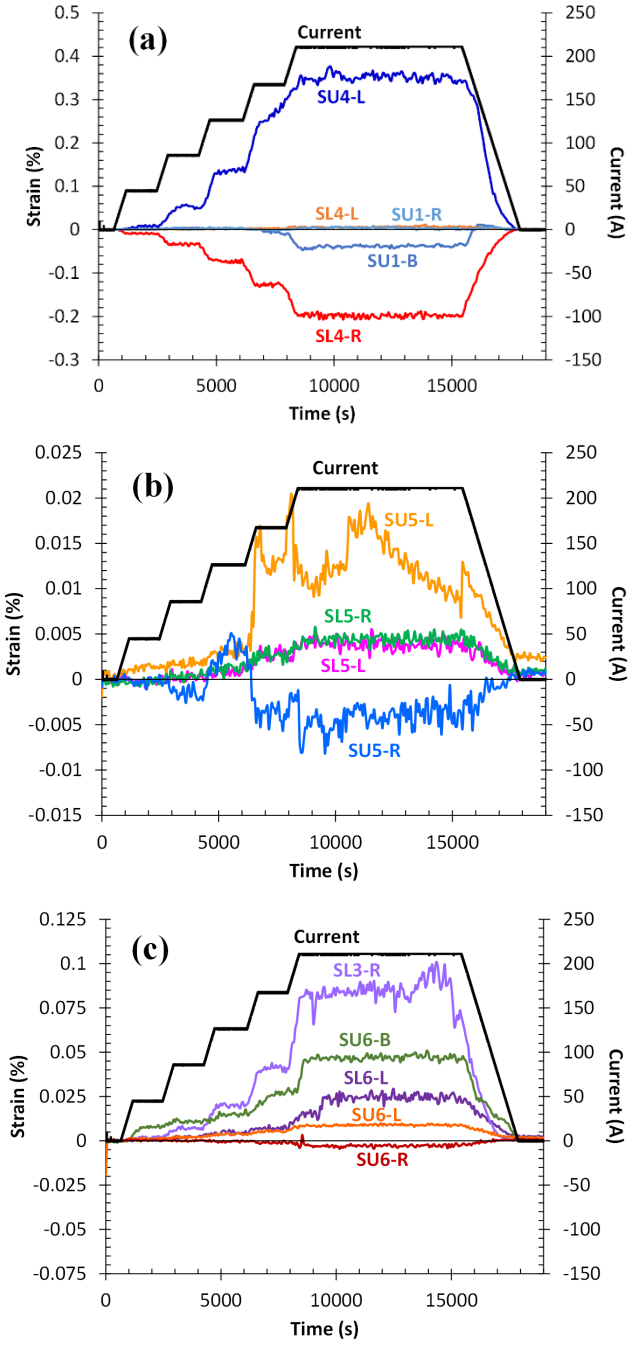

Fig. 5. Experimental results of strain on surface of sectors coils. (a) Sector coil #1, (b) Sector coil #2, (c) Sector coil #3.

IV. Numerical Simulation

A. Simulation model

We employed a three-dimensional mechanical simulation for metal-insulated and non-impregnated coils. The winding is not modeled as an integrated structure but rather as a discrete one. In an integrated model, the winding is considered as an anisotropic elastic body in both the circumferential and radial directions by applying the rule of mixture for composite materials [13]. However, in a discrete model, separation between windings is taken into account to allow movement of the REBCO tapes and co-winding SUS tapes, as depicted in Fig. 6. We took into account the laminated structure of REBCO tape and the contact between tapes by using gap element and contact element in finite element analysis. In this method, contact pairs are defined between adjacent turns in a pancake [10]. The mandrel and spacer plate were constructed from stainless steel. The mechanical properties of the materials used in this simulation are detailed in Table III. In the numerical structural simulation of REBCO coils, we considered the Lorentz forces generated by the magnetic fields of all main and sector coils. However, we did not account for the effect of screening current. [10-12].

During the cooling process, the components within a sector coil undergo shrinkage, which leads to the formation of gaps between the winding and the bobbin frame [14]. In this situation, stress cannot be effectively redistributed to the outer

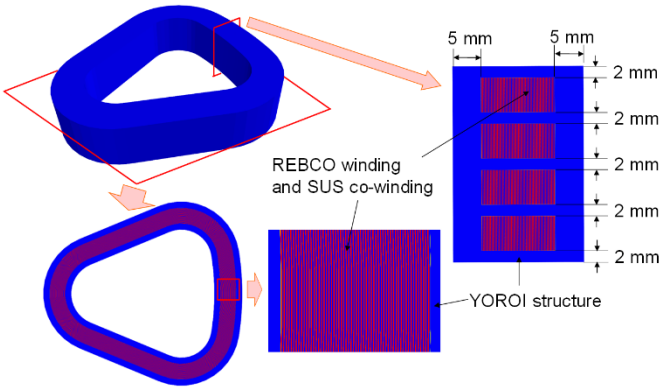

Fig. 6. Three-dimensional mechanical simulation model.

TABLE III
MECHANICAL PROPERTIES OF MATERIALS IN THIS SIMULATION [14]

Material	Young's modulus (GPa)	Poisson's Ratio	Mean linear thermal expansion (10^{-6} 1/K)
Stainless Steel	210	0.3	17.3
Hastelloy	221	0.32	12.8
Copper	138	0.35	16.8

frame, rendering the YOROI-coil structure less effective. The bobbin, upper and lower frames, and spacer between pancake coils are all constructed from stainless steel. The boundaries between the winding and the bobbin/frame are modeled as contact conditions. In the simulation of thermal stress, the coil is subjected to uniform cooling from 300 K to 30 K.

B. Simulation Results

Fig. 7 shows the simulation results of the longitudinal stress-strain on the coil winding at a current of 210 A. As shown in Fig. 7(a), the initial gap between the winding and the outer frame was 1.0 µm, and coil deformation was minimal. This result significantly deviates from the experimental results. Therefore, further analysis was conducted with different gap sizes between the winding and the outer frame. Fig. 7(b)-(d) display the results for gap sizes of 100 µm, 200 µm, and no outer frame, respectively. A gap of 100 µm is equivalent to the thickness of the REBCO tape. As the initial gap widens, the strain on the winding surface also increases. In the absence of an outer frame, meaning no YOROI structure, the strain on the sides of the straight section is -0.0008%, and the strain on the large curved section is 0.001%. These values are closer to the experimental results. At the current levels used in this experiment, it is unlikely that sufficient deformation occurred to fully utilize the benefits of the YOROI structure.

In the experiments, the strains were observed to be above the 0.3% degradation threshold, and there are two primary reasons for this observation:

1) The coil winding employs 6 mm wide REBCO wire. When strain is distributed in the width direction due to the screening current, it may result in additional strain at the point of strain gauge attachment.
2) Since it is a non-impregnated pancake coil, deformation occurs in the windings where the current leads are fixed. Furthermore, being a non-circular coil, the friction between the windings is not uniform during fabrication, cooling, and after excitation. Consequently, the deformation may not be evenly distributed throughout the entire coil but could be concentrated locally.

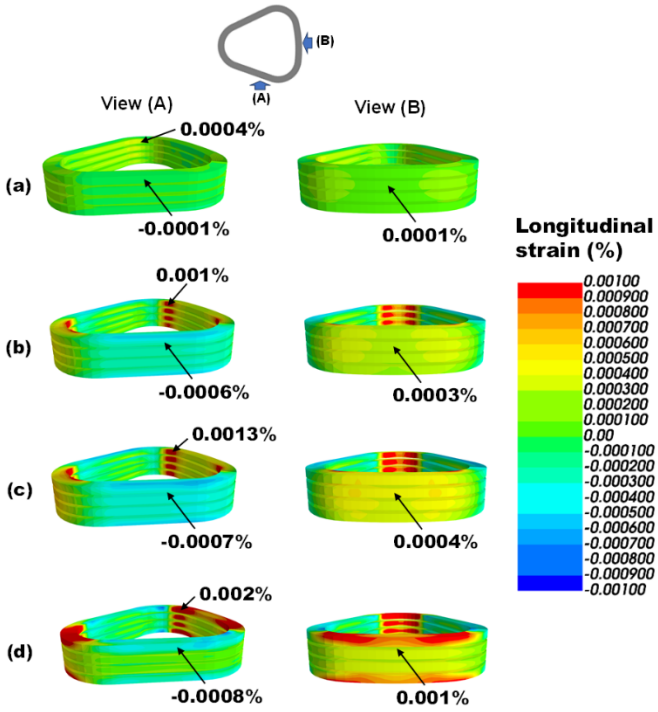

Fig. 7. Numerical results of strain on surface of sectors coils at a current of 210 A for a gap between winding and outer frame of (a) 1.0 µm, (b) 100 µm, (c) 200 µm and (d) no outer frame.

We are actively conducting simulations to further investigate and confirm these reasons.

V. SUMMARY

We designed and constructed the half-size demonstration NI-REBCO coil system, known as the Ultra-Baby Cyclotron, comprising three pairs of sector coils and four main split coils. In the summer of 2022, we started testing on the Ultra-Baby Cyclotron, measuring the mechanical deformation of the coils. Additionally, we conducted numerical simulations. The strain gauge behavior exhibited a mix of stability, instability, and large values, making it challenging to establish a consistent discussion. Some strains exceeded the wire degradation allowance of 0.3%, but we did not observe any coil degradation, such as an increase in voltage. We attempted to account for the large strain by considering the presence or absence of the outer YOROI frame, but the observed strains still appear to be excessively high. Moving forward, we plan to conduct an analysis to investigate the screening-current induced stress and deformation in the longitudinal direction of the winding in the non-impregnated pancake coil with the current leads fixed in ends. This analysis aims to provide a more comprehensive understanding of the observed strain behavior.

The experiment is still ongoing. We plan to increase the current to 540A, which is the assumed operating current, in order to measure larger deformations and gather more data for analysis.

REFERENCES

[1] C. Kratochwil, et al., “225Ac-PSMA-617 for PSMA targeting alpha-radiation therapy of patients with metastatic castration-resistant prostate cancer”, *Journal of Nuclear Medicine*, doi:10.2967/jnumed.116.178673 (2016).

[2] T. Watabe, et al.,” Enhancement of ^{211}At Uptake via the Sodium Iodide Symporter by the Addition of Ascorbic Acid in Targeted α-Therapy of Thyroid Cancer”, *Journal of Nuclear Medicine*, 60, 1301-1307. doi: 10.2967/jnumed.118.222638 (2019).

[3] H. Ueda, M. Fukuda, K. Hatanaka, T. Wang, X. Wang, A. Ishiyama, S. Noguchi, S. Nagaya, N. Kashima, N. Miyahara, “Conceptual Design of Next Generation HTS Cyclotron”, *IEEE Trans. Appl. Supercond.*, 23, 4100205 (2013)

[4] S. Hahn, D. K. Park, J. Bascuñán, Y. Iwasa, "HTS pancake coils without turn-to-turn insulation", *IEEE Trans. Appl. Supercond.*, Vol. 21, pp. 1592-1595 (2011).

[5] R. Kumagai, A. Ishiyama, H/ Ueda, S. Noguchi, T. Watanabe, M. Fukuda, G. Nishijima, J. Yoshida, “Fabrication and Experiments on a 1/2-Scale Demonstration NI-REBCO Coil System of a Skeleton Cyclotron for Cancer Therapy” *IEEE Trans. Appl. Supercond.* to be submitted.

[6] S. Nagaya, T. Watanabe, T. Tamada, M. Naruse, N. Kashima, T. Katagiri, N. Hirano, S. Awaji, H. Oguro and A. Ishiyama, " Development of high strength pancake coil with stress controlling structure by REBCO coated conductor", *IEEE Trans. Appl. Supercond*., vol. 23, no. 3, 2013, Art. no. 4601204.

[7] T. Watanabe, S. Nagaya, N. Hirano, S. Awaji, H. Oguro, Y. Tsuchiya, T. Omura, S. Nimori, T. Shimizu, A. Ishiyama, X. Wang, "Strengthening Effect of "Yoroi-Coil Structure" Against Electromagnetic Force," *IEEE Trans. Appl. Supercond.*, vol. 25, no. 3, 2015, Art. no. 8400204.

[8] X. Wang, H. Umeda, A. Ishiyama, M. Tashiro, H. Yamakawa, H. Ueda, T. Watanabe, S. Nagaya, “Development of Non-Circular REBCO Pancake Coil for High-Temperature Superconducting Cyclotron,” *IEEE Trans. Appl. Supercond.*, vol. 25, 2015, no. 3, Art. no. 4601904

[9] T. Watanabe, S. Nagaya, N. Hirano, S. Awaji, H. Oguro, A. Ishiyama, M. Hojo, M. Nishikawa, "Progress of "Yoroi-Coil Structure" in Mechanical Strength with High Current Density," *IEEE Trans. Appl. Supercond.*, vol. 27, no. 4, 2017, Art. no. 4602305.

[10] H. Ueda, et al. "Numerical evaluation of the deformation of REBCO pancake coil, considering winding tension, thermal stress, and screening-current-induced stress." *Supercond. Sci. Tech.* 34.2 (2021): 024003.

[11] J. Xia, et al. "Stress and strain analysis of a REBCO high field coil based on the distribution of shielding current." *Supercond. Sci. Tech.* 32.9 (2019): 095005.

[12] S. Takahashi, et al. "Hoop stress modification, stress hysteresis and degradation of a REBCO coil due to the screening current under external magnetic field cycling." *IEEE Trans. Appl. Supercond.* 30, 4 (2020): 19521694.

[13] X. Wang, A. Ishiyama, T. Tsujimura, H. Yamakawa, H. Ueda, T. Watanabe, S. Nagaya, " Numerical Structural Analysis on a New Stress Control Structure for High-Strength REBCO Pancake Coil," *IEEE Trans. Appl. Supercond.*, vol. 24, no. 3, 2014, Art. no. 4601605.

[14] H. Ueda, Y. Miyake, Y. Awazu, R. Inoue, SB. Kim, S. Noguchi, T. Watanabe, S. Nagaya, M. Fukuda and A. Ishiyama, “Numerical evaluation on electromagnetic and thermal stresses in non-circular REBCO pancake coils of multi-coil system for Skeleton Cyclotron”, *IEEE Trans. Appl. Supercond, IEEE Trans. Appl. Supercond.,* 31, 5, (2021) 4603705, doi: 10.1109/TASC.2021.3072871.